Second moment of the pion light-cone distribution amplitude from lattice QCD

V. M. Braun,[1] S. Collins,[1] M. Göckeler,[1] P. Pérez-Rubio,[1,*] A. Schäfer,[1] R. W. Schiel,[1] and A. Sternbeck[2,1]

[1]*Institut für Theoretische Physik, Universität Regensburg, 93040 Regensburg, Germany*

[2]*Theoretisch-Physikalisches Institut, Friedrich-Schiller-Universität Jena, 07743 Jena, Germany*

(Received 16 March 2015; published 20 July 2015)

We present the results of a lattice study of the second moment of the light-cone pion distribution amplitude using two flavors of dynamical (clover) fermions on lattices of different volumes and pion masses down to $m_\pi \sim 150$ MeV. At lattice spacings between 0.06 and 0.08 fm we find for the second Gegenbauer moment the value $a_2 = 0.1364(154)(145)$ at the scale $\mu = 2$ GeV in the $\overline{\rm MS}$ scheme, where the first error is statistical including the uncertainty of the chiral extrapolation, and the second error is the estimated uncertainty coming from the nonperturbatively determined renormalization factors. The error due to the continuum extrapolation cannot be quantified yet and is the only remaining significant source of uncertainty.

DOI: 10.1103/PhysRevD.92.014504 PACS numbers: 12.38.Gc, 13.60.Le, 14.40.Be

I. INTRODUCTION

Hard exclusive processes involving energetic pions in the final state are sensitive to the momentum fraction distribution of the valence quarks at small transverse separations, usually called the pion distribution amplitude (DA). Classical applications [1–3] have been to exclusive two-photon processes, e.g., the pion electromagnetic form factor at large momentum transfer and the transition form factor $\gamma^* \to \pi\gamma$. The latter process plays a very special role as the simplest hard exclusive reaction where QCD factorization can be tested at a quantitative level. It received a lot of interest recently, triggered by the partially conflicting measurements by *BABAR* [4] and BELLE [5] up to photon virtualities of the order of 40 GeV^2, see, e.g., [6–10]. Arguably, the most important application of the pion DA is currently the study of semileptonic weak decays $B \to \pi\ell\bar{\nu}_\ell$ at large recoil [11–13] using light-cone sum rules (LCSR) [14,15] and weak hadronic decays $B \to \pi\pi$ etc. in the framework of QCD factorization [16,17]. Both reactions contribute prominently to the determination of parameters of the quark mixing matrix in the Standard Model.

The precise definition of the pion DA $\phi_\pi(x,\mu^2)$ is based on the representation [1–3] as the matrix element of a nonlocal light-ray quark-antiquark operator. For example, for a positively charged pion

$$\langle 0|\bar{d}(z_2 n)\not{n}\gamma_5[z_2 n, z_1 n]u(z_1 n)|\pi(p)\rangle = if_\pi(p\cdot n)\int_0^1 dx e^{-i(z_1 x + z_2(1-x))p\cdot n}\phi_\pi(x,\mu^2), \quad (1)$$

where p^μ is the pion momentum, n^μ is a lightlike vector, $n^2 = 0$, $z_{1,2}$ are real numbers, $[z_2 n, z_1 n]$ is the Wilson line connecting the quark and the antiquark fields and $f_\pi = 132$ MeV is the usual pion decay constant. The DA $\phi_\pi(x,\mu^2)$ is scale dependent, which is indicated by the argument μ^2.

The physical interpretation of the variable x is that the u-quark carries the fraction x of the pion momentum, so that $1-x$ is the momentum fraction carried by the $\bar{d}$-antiquark. Neglecting isospin breaking effects and electromagnetic corrections the pion DA is symmetric under the interchange $x \leftrightarrow 1-x$:

$$\phi_\pi(x,\mu^2) = \phi_\pi(1-x,\mu^2). \quad (2)$$

Due to this symmetry, only the even moments involving the momentum fraction *difference*

$$\xi = x - (1-x) = 2x - 1 \quad (3)$$

carry nontrivial physical information:

$$\langle \xi^n \rangle = \int_0^1 dx (2x-1)^n \phi_\pi(x,\mu^2), \qquad n = 0, 2, \ldots. \quad (4)$$

The definition in (1) implies the normalization condition

$$\int_0^1 dx \phi_\pi(x,\mu^2) = 1. \quad (5)$$

A convenient parametrization of DAs is provided by the conformal expansion [18–20]. The underlying idea is to use the conformal symmetry of the QCD Lagrangian to separate transverse and longitudinal variables in the light-front pion wave function, similar in spirit to the partial-wave decomposition in quantum mechanics. The dependence on transverse coordinates is formulated as a scale dependence of the relevant operators and is

*Paula.Perez-Rubio@ur.de

governed by renormalization-group equations. The dependence on the longitudinal momentum fractions is described in terms of Gegenbauer polynomials $C_n^{3/2}(2x-1)$ which correspond to irreducible representations of the collinear conformal group $\mathrm{SL}(2,\mathbb{R})$. In this way one obtains

$$\phi_\pi(x,\mu^2) = 6x(1-x)\left[1 + \sum_{n=2,4,\ldots}^{\infty} a_n(\mu^2) C_n^{3/2}(2x-1)\right], \tag{6}$$

where all nonperturbative information is contained in the set of coefficients (Gegenbauer moments) $a_n(\mu_0^2)$ at a certain reference scale μ_0. To leading-logarithmic accuracy (LO), the Gegenbauer moments renormalize multiplicatively with the anomalous dimensions rising slowly with n. Thus the higher-order contributions in the Gegenbauer expansion are suppressed at large scales and asymptotically only the leading term survives,

$$\phi_\pi^{\mathrm{as}}(x) = 6x(1-x), \tag{7}$$

which is usually referred to as the asymptotic pion DA. It is widely accepted, however, that the pion DA deviates significantly from its asymptotic form at scales that can be achieved in experiments.

A particular model of the pion DA proposed by Chernyak and Zhitnitsky in 1982 [21] has played an important role in historic perspective. It was based on a calculation of a_2 using QCD sum rules [22], which resulted in a large value $a_2 \sim 0.5$–0.6 (at the scale 1 GeV), and the assumption that all higher-order coefficients can be neglected.

Since then, different approaches have been used: QCD sum rules with various improvements (e.g. [23–25]), LCSR-based analysis of experimental data on the pion electromagnetic and transition form factors (e.g. [7–9]) and weak B-meson decay form factors (e.g. [13]), lattice calculations [26,27] and recently also in the framework of Dyson-Schwinger equations [28]. A recent compilation of the existing results for a_2 can be found in Table I of Ref. [7].

Estimates of yet higher-order Gegenbauer coefficients are rather uncertain. A direct calculation of a_4 proves to be difficult and its extraction from the experimental data on, e.g., the pion transition form factor is complicated by the fact the LO contribution is proportional to the sum of Gegenbauer moments

$$\int_0^1 \frac{dx}{x}\phi_\pi(x,\mu^2) = 3[1 + a_2(\mu^2) + a_4(\mu^2) + \cdots]. \tag{8}$$

Thus, the values of $a_2(\mu^2)$ and $a_4(\mu^2)$ obtained in these extractions appear to be strongly correlated. The strong scaling violation in the pion transition form factor observed by *BABAR* [4] (but not confirmed by BELLE [5]) would imply a considerable enhancement of the pion DA close to the end points, meaning that the expansion in Gegenbauer polynomials is converging very slowly if at all, see the detailed discussion in [6,7,9]. The forthcoming upgrade of the Belle experiment and the KEKB accelerator [29], which aims to increase the experimental data set by a factor of 50, will allow one to measure transition form factors and related observables with unprecedented precision and resolve this issue. The question at stake is whether hard exclusive hadronic reactions are under theoretical control, which is highly relevant for all future high-intensity, medium energy experiments like, e.g., PANDA. On the theory side, several proposals exist how it might be possible to access DA moments beyond the second one (or the DA pointwise in x) on the lattice, e.g., [30,31], but the corresponding techniques are only in the exploratory stage.

In this paper we extend the lattice study [26] of the second moment of the pion DA by making use of a larger set of lattices with different volumes, lattice spacings and pion masses down to $m_\pi \sim 150$ MeV and implementing several technical improvements. We employ the variational approach with two and three interpolators to improve the signal from the pion state. The renormalization of the lattice data is performed nonperturbatively utilizing a version of the RI'-SMOM scheme. For the first time we include a nonperturbative calculation of the renormalization factor corresponding to the mixing with total derivatives, which proves to have a significant effect. Our main result is

$$a_2 = 0.1364(154)(145)(?) \tag{9}$$

for the second Gegenbauer moment of the pion DA, and

$$\langle \xi^2 \rangle = 0.2361(41)(39)(?). \tag{10}$$

Both numbers refer to the scale $\mu = 2$ GeV in the $\overline{\mathrm{MS}}$ scheme. The first error combines the statistical uncertainty and the uncertainty of the chiral extrapolation. The second error is the estimated uncertainty contributed by the nonperturbative determination of the renormalization and mixing factors. Our lattice data are collected for the lattice spacing $a = 0.06$–0.08 fm, and this range is not large enough to ensure a reliable continuum extrapolation for a_2 and $\langle \xi^2 \rangle$. The corresponding remaining uncertainty is indicated as (?). It has to be addressed in a future study.

The paper is organized as follows. In the next section we discuss the aspects of the continuum description of the pion DA that are relevant for our work. The basics of the lattice formulation are given in Sec. III. An important ingredient in our calculation is the nonperturbative evaluation of the renormalization and mixing coefficients, which is described in Sec. IV. The methods applied in the analysis of the bare data are detailed in Sec. V. Our results are presented in Sec. VI, followed by our conclusions and an outlook. In an Appendix we collect Tables V, VI, VII, VIII,

IX, and X of intermediate results for each gauge field ensemble used in our work.

II. MOMENTS OF THE PION DISTRIBUTION AMPLITUDE

The nonlocal operator in the expression for the pion DA (1) is defined as a generating function for renormalized leading-twist (i.e., twist two) local operators,

$$\bar{d}(z_2 n)\not{n}\gamma_5[z_2 n, z_1 n]u(z_1 n) = \sum_{k,l=0}^{\infty} \frac{z_2^k z_1^l}{k!l!} n^\rho n^{\mu_1} \ldots n^{\mu_{k+l}} \mathcal{M}^{(k,l)}_{\rho\mu_1\ldots\mu_{k+l}}, \tag{11}$$

where

$$\mathcal{M}^{(k,l)}_{\rho\mu_1\ldots\mu_{k+l}} = \bar{d}(0)\overleftarrow{D}_{(\mu_1}\ldots\overleftarrow{D}_{\mu_k}\vec{D}_{\mu_{k+1}}\ldots\vec{D}_{\mu_{k+l}}\gamma_{\rho)}\gamma_5 u(0). \tag{12}$$

Here D_μ is the covariant derivative and $(\cdots)$ denotes the symmetrization of all enclosed Lorentz indices and the subtraction of traces. The local operators $\mathcal{M}^{(k,l)}_{\rho\mu_1\ldots\mu_{k+l}}$ are assumed to be renormalized, e.g., in the $\overline{\text{MS}}$ scheme.

As a consequence, moments of the pion DA are given by matrix elements of local operators:

$$i^{k+l}\langle 0|\mathcal{M}^{(k,l)}_{\rho\mu_1\ldots\mu_{k+l}}|\pi(p)\rangle = i f_\pi p_{(\rho} p_{\mu_1}\ldots p_{\mu_{k+l})}\langle x^l(1-x)^k\rangle. \tag{13}$$

Neglecting isospin breaking effects and electromagnetic corrections one obtains the symmetry relation

$$\langle 0|\mathcal{M}^{(k,l)}_{\rho\mu_1\ldots\mu_{k+l}}|\pi(p)\rangle = \langle 0|\mathcal{M}^{(l,k)}_{\rho\mu_1\ldots\mu_{k+l}}|\pi(p)\rangle \tag{14}$$

and thus

$$\langle x^l(1-x)^k\rangle = \langle x^k(1-x)^l\rangle. \tag{15}$$

In addition, the product (Leibniz) rule for derivatives

$$\mathcal{M}^{(k+1,l)}_{\rho\mu_1\ldots\mu_{k+l+1}} + \mathcal{M}^{(k,l+1)}_{\rho\mu_1\ldots\mu_{k+l+1}} = \partial_{(\mu_{k+l+1}}\mathcal{M}^{(k,l)}_{\rho\mu_1\ldots\mu_{k+l})} \tag{16}$$

gives rise to the momentum-conservation constraint

$$\langle x^{l+1}(1-x)^k\rangle + \langle x^l(1-x)^{k+1}\rangle = \langle x^l(1-x)^k\rangle. \tag{17}$$

Specializing to the second moment, $l+k=2$, it is easy to see that only one independent matrix element remains, e.g.,

$$\langle\xi^2\rangle = 1 - 4\langle x(1-x)\rangle \tag{18}$$

or

$$a_2 = \frac{7}{18}\langle C_2^{3/2}(2x-1)\rangle = \frac{7}{12}[5\langle\xi^2\rangle - 1] = \frac{7}{3}[1 - 5\langle x(1-x)\rangle], \tag{19}$$

so that any moment $\langle\xi^2\rangle$, a_2, $\langle x(1-x)\rangle$ etc. can be used as a nonperturbative parameter to characterize the shape of the pion DA. Lacking any *a priori* information on the relative size of the different contributions, all such choices are equivalent. It is widely expected, however, that the numerical value of $\langle\xi^2\rangle$ is not far from 1/5 corresponding to the asymptotic pion DA (7). Hence, if

$$\langle\xi^2\rangle = \frac{1}{5} + \frac{12}{35}a_2 \tag{20}$$

is determined with a given accuracy at some reference scale μ_0 by a certain nonperturbative method, and a_2 is then obtained from the relation (20), the error on a_2 is strongly amplified by the subtraction of the asymptotic contribution. This effect is well known and has been observed in all calculations up to date. The error on a_2 is relevant as it propagates through the renormalization group equations. In other words, although using a_2 as a nonperturbative parameter instead of $\langle\xi^2\rangle$ for the pion DA at a low reference scale $\phi_\pi(x,\mu_0^2)$ is just a rewriting, this choice is much more adequate in order to describe the pion DA at high scales, $\phi_\pi(x,Q^2)$, $Q \gg \mu_0$, which enters QCD factorization theorems. Another issue to consider is that the relation in Eq. (16) and therefore (18), (19), (20) can be broken by lattice artifacts. Thus the choice of suitable operators requires some care. We will discuss our choice in more detail in the next section.

III. LATTICE FORMULATION

While the above relations refer to renormalized operators in Minkowski space, we now move to Euclidean space and define the bare operators

$$\begin{aligned}\mathcal{O}^-_{\rho\mu\nu}(x) &= \bar{d}(x)[\overleftarrow{D}_{(\mu}\overleftarrow{D}_\nu - 2\overleftarrow{D}_{(\mu}\vec{D}_\nu + \vec{D}_{(\mu}\vec{D}_\nu]\gamma_{\rho)}\gamma_5 u(x),\\ \mathcal{O}^+_{\rho\mu\nu}(x) &= \bar{d}(x)[\overleftarrow{D}_{(\mu}\overleftarrow{D}_\nu + 2\overleftarrow{D}_{(\mu}\vec{D}_\nu + \vec{D}_{(\mu}\vec{D}_\nu]\gamma_{\rho)}\gamma_5 u(x)\end{aligned} \tag{21}$$

as our operator basis. On the lattice the covariant derivatives will be replaced by their discretized versions.

The operator $\mathcal{O}^-_{\rho\mu\nu}$ can be written in a conventional shorthand notation as

$$\mathcal{O}^-_{\rho\mu\nu}(x) = \bar{d}(x)\overleftrightarrow{D}_{(\mu}\overleftrightarrow{D}_\nu\gamma_{\rho)}\gamma_5 u(x) \tag{22}$$

and its matrix element between the vacuum and the pion state is proportional to the bare lattice value of

$\langle (x-(1-x))^2\rangle = \langle \xi^2\rangle$. In the continuum, the operator $\mathcal{O}^+_{\rho\mu\nu}$ is the second derivative of the axial-vector current:

$$\mathcal{O}^+_{\rho\mu\nu}(x) = \partial_{(\mu}\partial_\nu \mathcal{O}_{\rho)}(x) \quad \text{with}$$
$$\mathcal{O}_\rho(x) = \bar d(x)\gamma_\rho\gamma_5 u(x). \tag{23}$$

However, this relation is violated on the lattice because of discretization errors in the derivatives. The distinction between $\mathcal{O}^+_{\rho\mu\nu}$ and $\partial_{(\mu}\partial_\nu\mathcal{O}_{\rho)}$ for finite lattice spacing appears to be numerically important and will be discussed in detail in what follows. Note that $\mathcal{O}^+$ is the Euclidean analogue of the Minkowski-space operator $\mathcal{M}^{(0,2)} + 2\mathcal{M}^{(1,1)} + \mathcal{M}^{(2,0)}$ such that its matrix element between the vacuum and the pion state corresponds to the bare value of $\langle (x+1-x)^2\rangle = \langle 1^2\rangle$.

The corresponding renormalized (e.g., in the $\overline{\rm MS}$ scheme) axial-vector current is then given by

$$\mathcal{O}^{\overline{\rm MS}}_\rho(x) = Z_A \mathcal{O}_\rho(x) \tag{24}$$

with $Z_A \neq 1$ on the lattice.

In order to express its matrix elements in terms of the physical quantities introduced in Minkowski space we apply the rules

$$\gamma^0_{\rm M} = \gamma_4, \qquad \gamma^j_{\rm M} = i\gamma_j \tag{25}$$

for $j = 1,2,3$, where the subscript M distinguishes the Minkowski objects. Consequently,

$$\gamma^{\rm M}_5 = i\gamma^0_{\rm M}\gamma^1_{\rm M}\gamma^2_{\rm M}\gamma^3_{\rm M} = -\gamma_1\gamma_2\gamma_3\gamma_4 = -\gamma_5. \tag{26}$$

The components of the three-vector $\mathbf{p}$ of the spatial momentum of the pion will be denoted by p_j, although they are equal to the contravariant space components of the Minkowski momentum p. The time component of the Minkowski momentum is identified with the corresponding energy: $p_0 = E_\pi(\mathbf{p})$. In this way one gets in Euclidean notation

$$\langle 0|\mathcal{O}^{\overline{\rm MS}}_4(0)|\pi(\mathbf{p})\rangle = -iE_\pi(\mathbf{p})f_\pi, \tag{27}$$

$$\langle 0|\mathcal{O}^{\overline{\rm MS}}_j(0)|\pi(\mathbf{p})\rangle = -p_j f_\pi. \tag{28}$$

Similarly, the Euclidean space components of the coordinate vector x are identified with the contravariant components of the Minkowski space-time four-vector, while for the time components we have $x_0 = -ix_4$. This entails the following rule for the covariant derivatives:

$$-iD^{\rm M}_0 = D_4, \qquad D^{\rm M}_j = D_j. \tag{29}$$

Therefore we find, e.g., for $j \neq k$

$$\langle 0|\mathcal{O}^{\overline{\rm MS}-}_{4jk}(0)|\pi(\mathbf{p})\rangle = if_\pi\langle\xi^2\rangle E_\pi(\mathbf{p})p_j p_k. \tag{30}$$

The operators $\mathcal{O}^-_{\rho\mu\nu}$ and $\mathcal{O}^+_{\rho\mu\nu}$ mix under renormalization even in the continuum. On the lattice the continuous rotational $O(4)$ symmetry of Euclidean space is broken and reduced to the discrete $H(4)$ symmetry of the hypercubic lattice. This symmetry breaking can introduce additional mixing operators. It can even lead to mixing of the operators of interest with operators of lower dimension such that the mixing coefficients are proportional to powers of $1/a$. This complicates the renormalization procedure significantly. However, it may be possible to choose the lattice operators such that they belong to an irreducible representation of $H(4)$ which forbids mixing with further operators, in particular with lower-dimensional operators. In the present case there is one such choice, given by the operators $\mathcal{O}^\pm_{\rho\mu\nu}$ with all three indices different. For the computation of the required matrix elements we can restrict ourselves to the operators (see, e.g., [26,27])

$$\mathcal{O}^\pm_{4jk}, \qquad j \neq k \in \{1,2,3\}. \tag{31}$$

The renormalized operators are then given by

$$\mathcal{O}^{\overline{\rm MS}-}_{4jk}(x) = Z_{11}\mathcal{O}^-_{4jk}(x) + Z_{12}\mathcal{O}^+_{4jk}(x),$$
$$\mathcal{O}^{\overline{\rm MS}+}_{4jk}(x) = Z_{22}\mathcal{O}^+_{4jk}(x). \tag{32}$$

Note that due to the discretization artifacts in the derivatives one cannot expect Z_{22} to be equal to Z_A.

For the calculation of $\langle\xi^2\rangle^{\overline{\rm MS}}$ and $a_2^{\overline{\rm MS}}$ we are now left with two tasks: computation of the bare matrix elements and evaluation of the renormalization factors. We extract the bare matrix elements from two-point correlation functions of the operators $\mathcal{O}^\pm_{\rho\mu\nu}$ and $\mathcal{O}_\rho$ with suitable interpolating fields $J(x)$ for the π-mesons. For the latter we consider the two possibilities

$$J_5(x) = \bar u(x)\gamma_5 d(x),$$
$$J_{45}(x) = \bar u(x)\gamma_4\gamma_5 d(x) \tag{33}$$

with smeared quark fields. The details of our smearing algorithm will be given below. Let

$$C^A_\rho(t,\mathbf{p}) = a^3\sum_{\mathbf{x}} e^{-i\mathbf{p}\cdot\mathbf{x}}\langle \mathcal{O}_\rho(\mathbf{x},t)J_A(0)\rangle,$$
$$C^{\pm;A}_{\rho\mu\nu}(t,\mathbf{p}) = a^3\sum_{\mathbf{x}} e^{-i\mathbf{p}\cdot\mathbf{x}}\langle \mathcal{O}^\pm_{\rho\mu\nu}(\mathbf{x},t)J_A(0)\rangle, \tag{34}$$

where $A = 5$ or $A = 45$, $\mathbf{p}$ is the three-vector of the spatial momentum, and the summation goes over the set of spatial lattice points $\mathbf{x}$ for a given Euclidean time t.

For times t, where the correlation functions are saturated by the contribution of the lowest-mass pion state, we expect that, e.g.,

$$C^{\pm;A}_{\rho\mu\nu}(t,\mathbf{p}) = \langle 0|\mathcal{O}^{\pm}_{\rho\mu\nu}(0)|\pi(\mathbf{p})\rangle\langle\pi(\mathbf{p})|J_A(0)|0\rangle \times \frac{1}{2E}[e^{-Et} + \tau_{\mathcal{O}}\tau_J e^{-E(T-t)}]. \quad (35)$$

Here $E \equiv E_\pi(\mathbf{p})$, T is the temporal extent of our lattice, and the τ-factors take into account transformation properties of the correlation functions under time reversal. One finds $\tau_{J_5} = -1$, $\tau_{J_{45}} = 1$, $\tau_{\mathcal{O}} = 1$ for the operators $\mathcal{O}^{\pm}_{4jk}$, $\mathcal{O}_4$ and $\tau_{\mathcal{O}} = -1$ for $\mathcal{O}_j$, where $j,k = 1,2,3$. We utilize these symmetries in order to reduce the statistical fluctuations of our raw data, i.e., we average over the two corresponding times t and $T-t$ with the appropriate sign factors.

From the ratios

$$\mathcal{R}^{\pm;A}_{\rho\mu\nu;\sigma} = \frac{C^{\pm;A}_{\rho\mu\nu}(t,\mathbf{p})}{C^{A}_{\sigma}(t,\mathbf{p})} \quad (36)$$

we can extract the required bare matrix elements $\langle 0|\mathcal{O}^{\pm}_{\rho\mu\nu}(0)|\pi(\mathbf{p})\rangle$, which carry the information on the second moment of the pion DA.

Equation (30) shows that a calculation of matrix elements of $\mathcal{O}^{\pm}_{4jk}$ requires two nonvanishing spatial components of the momentum. We choose them as small as possible, $p = 2\pi/L$, where L is the spatial extent of our lattice. To suppress statistical fluctuations we average over the possible directions, e.g., $\mathbf{p} = (p,p,0)$, $\mathbf{p} = (p,-p,0)$, $\mathbf{p} = (-p,p,0)$, $\mathbf{p} = (-p,-p,0)$ for $j = 1$, $k = 2$. If the correlation functions are dominated by the single-pion states, the time-dependent factors in the ratios of correlation functions cancel and we obtain, e.g., for the operator $\mathcal{O}^{\pm}_{412}$ and the momentum $\mathbf{p} = (p,p,0)$

$$\mathcal{R}^{\pm;A}_{412;4} = -\left(\frac{2\pi}{L}\right)^2 R^{\pm}, \quad (37)$$

where the constants $R^{\pm}$ are related to the bare lattice values of the second moment of the pion DA through

$$\langle\xi^2\rangle^{\text{bare}} = R^-, \qquad a_2^{\text{bare}} = \frac{7}{12}(5R^- - R^+). \quad (38)$$

They should not depend on the choice of the interpolating field J_A. Note that $R^+ \neq 1$ and therefore for bare quantities

$$a_2^{\text{bare}} \neq \frac{7}{12}(5\langle\xi^2\rangle^{\text{bare}} - 1). \quad (39)$$

For the renormalized moments in the $\overline{\text{MS}}$ scheme we obtain

$$\langle\xi^2\rangle^{\overline{\text{MS}}} = \zeta_{11}R^- + \zeta_{12}R^+, \qquad a_2^{\overline{\text{MS}}} = \frac{7}{12}[5\zeta_{11}R^- + (5\zeta_{12} - \zeta_{22})R^+], \quad (40)$$

where

$$\zeta_{11} = \frac{Z_{11}}{Z_A}, \qquad \zeta_{12} = \frac{Z_{12}}{Z_A}, \qquad \zeta_{22} = \frac{Z_{22}}{Z_A} \quad (41)$$

are ratios of renormalization constants defined in the next section.

In the continuum limit we expect that

$$Z_{22}\langle 0|\mathcal{O}^{+}_{4jk}(0)|\pi(\mathbf{p})\rangle = -Z_A p_j p_k \langle 0|\mathcal{O}_4(0)|\pi(\mathbf{p})\rangle = ip_j p_k E_\pi(\mathbf{p}) f_\pi. \quad (42)$$

Hence the quantity

$$\langle 1^2\rangle^{\overline{\text{MS}}} := \frac{Z_{22}}{Z_A}\frac{\langle 0|\mathcal{O}^{+}_{4jk}(0)|\pi(\mathbf{p})\rangle}{(-p_j p_k)\langle 0|\mathcal{O}_4(0)|\pi(\mathbf{p})\rangle} = \zeta_{22}R^+ \quad (43)$$

should approach unity as the lattice spacing tends to zero. In this case the relation

$$a_2^{\overline{\text{MS}}} = \frac{7}{12}(5\langle\xi^2\rangle^{\overline{\text{MS}}} - 1) \quad (44)$$

is recovered [cf. Eq. (19)], whereas for finite lattice spacing it follows from (40)

$$a_2^{\overline{\text{MS}}} = \frac{7}{12}(5\langle\xi^2\rangle^{\overline{\text{MS}}} - \langle 1^2\rangle^{\overline{\text{MS}}}). \quad (45)$$

We emphasize that Eq. (44) is only recovered in the continuum limit, which is always delicate. There are two possibilities: Either $\langle\xi^2\rangle$ is measured on the lattice, the result extrapolated to zero lattice spacing, and at the final step a_2 is obtained using the relation (44), or a_2 is calculated directly on the lattice and then extrapolated to the continuum limit. The first approach was used in Refs. [26,27] whereas in this paper we use the second method.

IV. RENORMALIZATION CONSTANTS

From our bare matrix elements we have to compute the corresponding renormalized matrix elements in the $\overline{\text{MS}}$ scheme, which is used in the perturbative calculations. In the continuum we therefore have to deal with the renormalization of the two mixing operator multiplets given in Eq. (21). Note that $\mathcal{O}^{+}_{\rho\mu\nu}$, being the second derivative of the axial-vector current, has vanishing forward matrix elements, at least in the continuum.

On the lattice we work with the operator multiplets

$$\mathcal{O}^{+}_{423}, \qquad \mathcal{O}^{+}_{413}, \qquad \mathcal{O}^{+}_{412}, \qquad \mathcal{O}^{+}_{123} \quad (46)$$

and

$$\mathcal{O}^{-}_{423}, \qquad \mathcal{O}^{-}_{413}, \qquad \mathcal{O}^{-}_{412}, \qquad \mathcal{O}^{-}_{123}. \quad (47)$$

Under the hypercubic group $H(4)$, both multiplets transform identically according to a four-dimensional irreducible

representation [32]. The symmetry properties of these multiplets ensure that they do not mix with any other operators. Because of the well-known shortcomings of lattice perturbation theory we want to determine the renormalization and mixing factors nonperturbatively on the lattice, utilizing a variant of the RI'-MOM scheme. However, since forward matrix elements of $\mathcal{O}^+_{\rho\mu\nu}$ eventually vanish, we cannot use the momentum geometry of the original RI'-MOM scheme but have to work with a kind of RI'-SMOM scheme [33].

In order to describe our renormalization procedure we consider a somewhat more general situation than what is needed in this paper. Let $\mathcal{O}_i^{(m)}(x)$ $(i = 1, 2, \ldots, d,$ $m = 1, 2, \ldots, M)$ denote M multiplets of local quark-antiquark operators which transform identically according to some irreducible, unitary, d-dimensional representation of $H(4)$. Call the unrenormalized, but (lattice-)regularized vertex functions (in the Landau gauge) $V_i^{(m)}(p, q)$, where p and q are the external quark momenta. The corresponding renormalized (in the $\overline{\rm MS}$ scheme) vertex functions are denoted by $\bar{V}_i^{(m)}(p, q)$. The dependence of $\bar{V}_i^{(m)}$ on the renormalization scale μ is suppressed for brevity. Note that $V_i^{(m)}$ carries Dirac indices and is therefore to be considered as a 4×4-matrix. (The color indices have been averaged over.)

We choose

$$p = \frac{\mu}{\sqrt{2}}(1, 1, 0, 0), \qquad q = \frac{\mu}{\sqrt{2}}(0, 1, 1, 0) \tag{48}$$

such that $p^2 = q^2 = (p - q)^2 = \mu^2$. As our renormalization condition we take (in the chiral limit)

$$\sum_{i=1}^{d} \mathrm{tr}(\hat{B}_i^{(m)} \hat{B}_i^{(m')\dagger}) = Z_q^{-1} \sum_{m''=1}^{M} \hat{Z}_{mm''} \sum_{i=1}^{d} \mathrm{tr}(V_i^{(m'')} \hat{B}_i^{(m')\dagger}), \tag{49}$$

where $\hat{B}_i^{(m)}$ is the lattice Born term corresponding to $V_i^{(m)}$. The wave function renormalization constant of the quark fields Z_q is determined from the quark propagator, as usual [34], and subsequently converted to the $\overline{\rm MS}$ scheme. Using the lattice Born term instead of the continuum Born term and proceeding analogously in the calculation of Z_q ensures that $\hat{Z}$ is the unit matrix in the free case.

The renormalization matrix $\hat{Z}$ leads from the bare operators on the lattice to renormalized operators in our SMOM scheme. The matrix Z transforming the bare operators into renormalized operators in the $\overline{\rm MS}$ scheme is then given by $Z = C\hat{Z}$, where the matrix C is defined as

$$\sum_{m''=1}^{M} \sum_{i=1}^{d} C_{mm''} \mathrm{tr}(B_i^{(m'')} B_i^{(m')\dagger}) = \sum_{i=1}^{d} \mathrm{tr}(\bar{V}_i^{(m)} B_i^{(m')\dagger}). \tag{50}$$

Here $\bar{V}_i^{(m)}$ is the renormalized vertex function in the $\overline{\rm MS}$ scheme and $B_i^{(m)}$ is the continuum Born term such that the conversion matrix C is completely determined from a continuum calculation.

Here we have to consider the cases $M = 2$, $d = 4$ for the multiplets (46), (47) and $M = 1$, $d = 4$ for the axial-vector current. The required $\overline{\rm MS}$ vertex functions in the chiral limit for up to two loops can be extracted from Refs. [35,36]. As we are only interested in ratios of renormalization factors, Z_q drops out and is not needed. In the following we describe our method for the determination of the renormalization matrix of the multiplets (46), (47). The procedure for the ratios with Z_A is completely analogous, because the anomalous dimension of the nonsinglet axial-vector current vanishes.

The calculation of the vertex functions with the help of momentum sources is straightforward. Partially twisted boundary conditions applied to the quark propagators allow us to vary the renormalization scale μ independently of the lattice size. The ensembles used for the evaluation of the Z matrices according to the above formulas are listed in Table I. Due to the rather small quark masses the subsequent chiral extrapolation appears to be quite safe.

Ideally, the renormalization scale μ should satisfy the conditions

$$1/L^2 \ll \Lambda^2_{\rm QCD} \ll \mu^2 \ll 1/a^2 \tag{51}$$

for a lattice with lattice spacing a and extent L. Then lattice artifacts would be negligible and the scale dependence could be described by low-order continuum perturbation theory. However, the above conditions are hard to realize in practice and the Z-values at any given scale suffer from discretization artifacts as well as from truncation errors of the perturbative expansions. Therefore we try to exploit as much of the available nonperturbative information as possible by performing a joint fit of the μ-dependence of the chirally extrapolated renormalization matrices $Z(a, \mu)_{\rm MC}$ for our three β-values $\beta = 5.20$, 5.29 and 5.40.

TABLE I. Ensembles used for nonperturbative renormalization. For pion masses and lattice spacings in physical units see Table IV.

β	κ	Size
5.20	0.13550	$32^3 \times 64$
5.20	0.13584	$32^3 \times 64$
5.20	0.13596	$32^3 \times 64$
5.29	0.13620	$32^3 \times 64$
5.29	0.13632	$32^3 \times 64$
5.29	0.13640	$64^3 \times 64$
5.40	0.13640	$32^3 \times 64$
5.40	0.13647	$32^3 \times 64$
5.40	0.13660	$48^3 \times 64$

The choice of the fitting procedure is motivated by the following considerations. The (perturbative) running of the Z-matrices is governed by the anomalous dimension matrix

$$\gamma = -\left(\mu \frac{dZ}{d\mu}\right) Z^{-1}. \tag{52}$$

Introducing the running renormalized coupling $g(\mu)$ with $\mu\, dg/d\mu = \beta(g)$ we get

$$\frac{dZ}{dg} = -\frac{\gamma(g)}{\beta(g)} Z. \tag{53}$$

This system of differential equations can formally be solved in the form

$$Z(\mu)Z^{-1}(\mu_0) = \sum_{n=0}^{\infty} (-1)^n \int_{g(\mu_0)}^{g(\mu)} dg_n \int_{g(\mu_0)}^{g_n} dg_{n-1} \cdots \times \int_{g(\mu_0)}^{g_2} dg_1 \frac{\gamma(g_n)}{\beta(g_n)} \cdots \frac{\gamma(g_2)}{\beta(g_2)} \frac{\gamma(g_1)}{\beta(g_1)}. \tag{54}$$

From the three-loop anomalous dimension matrix one can calculate a corresponding approximation of $W(\mu, \mu_0) \coloneqq Z(\mu)Z^{-1}(\mu_0)$, which should describe the μ-dependence for sufficiently large scales μ if there were no discretization effects. Adding a plausible ansatz for an effective description of these lattice artifacts we arrive at the following fit function for the matrices $Z(a,\mu)_{\mathrm{MC}}$:

$$Z(a,\mu)_{\mathrm{MC}} = W(\mu,\mu_0) Z(a,\mu_0) + A_1 a^2\mu^2 + A_2 (a^2\mu^2)^2 + A_3 (a^2\mu^2)^3. \tag{55}$$

The fit parameters are the entries of the three renormalization matrices $Z(a,\mu_0)$ at the reference scale μ_0 and the entries of the three matrices A_i parametrizing the lattice artifacts. Note that we allow for a nonvanishing value of Z_{21} although Z_{21} vanishes in the continuum.

The statistical errors of the data are quite small, in particular for larger scales, and the resulting statistical errors of the fit parameters turn out to be unrealistically tiny. Therefore the statistical errors will be ignored in the following. The systematic uncertainties, on the other hand, are much more important. In order to estimate them we perform a number of fits varying exactly one element of the analysis at a time. More precisely, we choose as representative examples for fit intervals $4\ \mathrm{GeV}^2 < \mu^2 < 100\ \mathrm{GeV}^2$ and $2\ \mathrm{GeV}^2 < \mu^2 < 30\ \mathrm{GeV}^2$, and we use the expressions for the $\overline{\mathrm{MS}}$ vertex functions $\bar{V}_i^{(m)}$ with $n_{\mathrm{loops}} = 1, 2$. For the parametrization of the lattice artifacts we either take the complete expression in Eq. (55) or we set $A_3 = 0$. Finally, we consider values for r_0 and $r_0\Lambda_{\overline{\mathrm{MS}}}$ corresponding to the results given in Ref. [37]. The various possibilities are compiled in Table II.

TABLE II. Choices for the fits.

Fit number	Fit interval (in GeV^2)	n_{loops}	Lattice artifacts	r_0 (in fm)	$r_0\Lambda_{\overline{\mathrm{MS}}}$
1	$4 < \mu^2 < 100$	2	$A_3 \neq 0$	0.50	0.789
2	$2 < \mu^2 < 30$	2	$A_3 \neq 0$	0.50	0.789
3	$4 < \mu^2 < 100$	1	$A_3 \neq 0$	0.50	0.789
4	$4 < \mu^2 < 100$	2	$A_3 = 0$	0.50	0.789
5	$4 < \mu^2 < 100$	2	$A_3 \neq 0$	0.49	0.789
6	$4 < \mu^2 < 100$	2	$A_3 \neq 0$	0.50	0.737

TABLE III. Fit results at $\beta = 5.40$ for $\mu_0^2 = 4\ \mathrm{GeV}^2$.

	Fit 1	Fit 2	Fit 3	Fit 4	Fit 5	Fit 6
ζ_{11}	2.026	2.031	2.123	2.001	2.040	2.041
ζ_{12}	−0.199	−0.205	−0.233	−0.188	−0.202	−0.203
ζ_{22}	1.474	1.476	1.479	1.467	1.474	1.474

As an example we show the fit results for $\beta = 5.40$ in Table III, choosing $\mu_0^2 = 4\ \mathrm{GeV}^2$. The numbers for the other β-values are similar.

The largest effect comes from the variation of n_{loops}: Working with the one-loop vertex functions increases the result for ζ_{11} by about 5%, and the modulus of the mixing coefficient ζ_{12} increases even by about 17%. In order to obtain our final numbers for $\langle \xi^2 \rangle^{\overline{\mathrm{MS}}}$, $a_2^{\overline{\mathrm{MS}}}$ and $\langle 1^2 \rangle^{\overline{\mathrm{MS}}}$ we extract them from the raw data for $R^{\pm}$ using each of these sets of values for ζ_{11}, ζ_{12} and ζ_{22}. So we get six results for each of our gauge field ensembles. As our central values we take the results from fit 1. Defining δ_i as the difference between the result obtained with the ζs from fit i and the result determined with the ζs from fit 1, we estimate the systematic uncertainties due to the renormalization factors as $\sqrt{\delta_2^2 + (0.5 \cdot \delta_3)^2 + \delta_4^2 + \delta_5^2 + \delta_6^2}$. Here we have multiplied δ_3 by $1/2$, because going from two loops to three or more loops in the perturbative vertex functions is expected to lead to a smaller change than going from one loop to two loops. This should amount to a rather conservative error estimate.

In Fig. 1 we show the entries of the matrix

$$W^{-1}(\mu,\mu_0) Z(a,\mu)_{\mathrm{MC}} = Z(a,\mu_0) + W^{-1}(\mu,\mu_0) \times [A_1 a^2\mu^2 + A_2 (a^2\mu^2)^2 + A_3 (a^2\mu^2)^3] \tag{56}$$

for $\mu_0^2 = 4\ \mathrm{GeV}^2$ at our three β-values along with the fit curves resulting from fit 1 in Table II. The horizontal lines represent the fitted values $\zeta_{11}(a,\mu_0)$ etc.

In the previous paper [26] the renormalization and mixing factors were evaluated in a mixed perturbative-nonperturbative approach, based on the representation of $\mathcal{O}^+_{\rho\mu\nu}$ as the second derivative of the axial-vector current

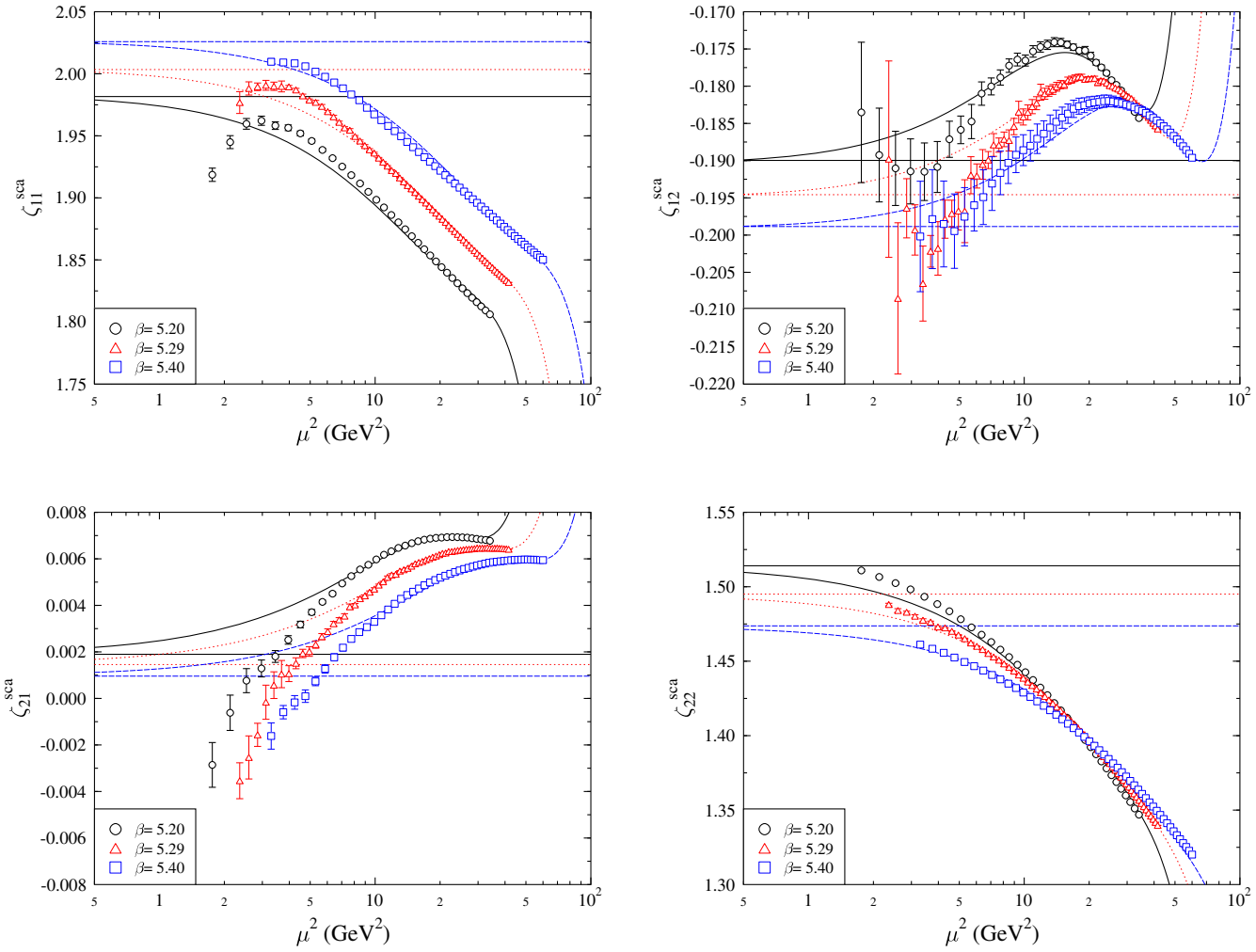

FIG. 1 (color online). Renormalization and mixing factors ζ_{ij} in the chiral limit, perturbatively scaled to $\mu_0 = 2$ GeV [cf. Eq. (56)] together with curves representing fit 1. The error bars show the statistical errors. The horizontal lines indicate the fitted values $\zeta_{ij}(a, \mu_0)$. Note that the fit is aimed at describing the data for large values of the scale μ, the fit interval being 4 GeV$^2 < \mu^2 < 100$ GeV^2.

[see Eq. (23)]. Repeating this calculation in a completely nonperturbative setting we find that the overall renormalization factor corresponding to ζ_{11} agrees within a few percent. The nonperturbative mixing coefficient, on the other hand, has the same (negative) sign as its perturbatively computed counterpart, but its modulus is up to 1 order of magnitude larger. This observation underlines the necessity of nonperturbative renormalization, at least for the presently reachable β-values.

V. ANALYSIS OF THE BARE DATA

As was already mentioned in Sec. III, the bare matrix elements related to the pion DA's second moments can be extracted from ratios of lattice correlation functions given by Eq. (36). We briefly describe our procedure.

The gauge field configurations used in this paper have been generated with the Wilson gauge action and $n_f = 2$ flavors of nonperturbatively improved Wilson fermions. We have analyzed O(1000–2000) configurations for three different values of the gauge coupling, $\beta = 5.20, 5.29, 5.40$, and pion masses in the range $m_\pi \sim 500$–150 MeV. The lattice spacings and spatial volumes vary between 0.06–0.081 fm and (1.71–4.57 fm)^3, respectively. A list of our ensembles can be found in Table IV. For scale setting we used the Sommer parameter with the value $r_0 = 0.5$ fm [37,38].

The correlation functions (34) have been computed for the operators $\mathcal{O}_4, \mathcal{O}_{4jk}$ [see Eq. (31)] leading to the ratios $\mathcal{R}_{4jk;4}^{\pm;J_{\rm opt}}$, where $J_{\rm opt}$ is discussed below. On most of the ensembles, we performed more than one measurement per configuration to increase the statistics. The source positions for the correlation functions were selected randomly to reduce the autocorrelations among configurations lying close to one another in the Monte Carlo history. We want the interpolating operators to have a good overlap with the ground state of the pion. To this end, Wuppertal smearing [39,40] was applied to the sources, with APE smeared [41] gauge fields.

In order to reduce the overlap with excited states even further we have used the variational method [42–45] with

TABLE IV. Ensembles used for this paper. The number of measurements per configuration is shown in parentheses.

κ	m_π/ MeV	Size	$m_\pi L$	Number of configurations
	$\beta = 5.20, a = 0.081$ fm, $a^{-1} = 2400$ MeV			
0.13596[a]	280	$32^3 \times 64$	3.7	1999(×4)
	$\beta = 5.29, a = 0.071$ fm, $a^{-1} = 2800$ MeV			
0.13620[a]	430	$24^3 \times 48$	3.7	1764(×2)
0.13620[a]	422	$32^3 \times 64$	4.8	1998(×2)
0.13632	294	$32^3 \times 64$	3.4	1999(×1)
0.13632	289	$40^3 \times 64$	4.2	2028(×2)
0.13632[a]	285	$64^3 \times 64$	6.7	1237(×2)
0.13640[a]	150	$64^3 \times 64$	3.5	1599(×3)
	$\beta = 5.40, a = 0.060$ fm, $a^{-1} = 3300$ MeV			
0.13640	491	$32^3 \times 64$	4.8	982(×2)
0.13647[a]	430	$32^3 \times 64$	4.2	1999(×2)
0.13660	260	$48^3 \times 64$	3.8	2178(×2)

[a]These ensembles were generated on the QPACE systems, financed primarily by the SFB/TR 55, while the others were generated earlier within the QCDSF collaboration.

the two interpolators (33) to obtain an optimal interpolator $J_{\rm opt} = \alpha J_5 + \beta J_{45}$. This procedure is based on the t-dependent 2×2-matrix of two-point correlation functions of the interpolating fields J_5 and J_{45}, projected onto vanishing spatial momentum. Solving a generalized eigenvalue problem for this matrix allows one to determine $J_{\rm opt}$ from the eigenvector belonging to the lowest energy eigenvalue. Using this interpolator in the correlation functions improves the signal of the ground state. We have also tried to apply the additional interpolators method with a third, time-shifted interpolator [46,47], but the results changed only marginally. Our final numbers will be based on the results obtained with $J_{\rm opt}$. This differs from the approach of Ref. [26], where only the interpolator J_5 was utilized in the final analysis.

To suppress statistical fluctuations, we have averaged over all possible values of j, k, and all possible momentum directions,

$$R_{\rm av}^{\pm} = \left(\frac{L}{2\pi}\right)^2 \frac{1}{12} \sum_j \sum_{k>j} \sum_{p_j=\pm p} \sum_{p_k=\pm p} |\mathcal{R}_{4jk;4}^{\pm;J_{\rm opt}}|, \qquad (57)$$

where $p = 2\pi/L$. The quantities $R_{\rm av}^{\pm}$ have then been fitted to a constant in a time interval where a plateau could be identified. The choice of the fit ranges was based on the goodness of the correlated χ^2-values and the stability of the results upon reducing the fit interval. The statistical errors were evaluated using the jackknife procedure combined with the binning method. We have observed that a binsize $n_{\rm bin} = 4$ saturates the statistical error, which means that the autocorrelations are satisfactorily taken into account.

Our bare results are collected in Tables V, VI, and VII in the Appendix. Comparing the errors in Table VII to those in Tables V, VI, one gets an impression of the benefit of employing the variational method. In Fig. 2 we display $R_{\rm av}^{-} = \langle \xi^2 \rangle^{\rm bare}$ for the two interpolating operators J_{45} and J_5 together with the corresponding results obtained in Ref. [26]. We observe that our data are consistent with the measurements in [26], but extend to considerably smaller pion masses all the way down to the physical value. Nevertheless, in the next section we will see that taking into account Eq. (39) and using the nonperturbatively computed value of ζ_{12} leads to a significant shift in the final result.

VI. RENORMALIZED RESULTS

In this section we present our results for the renormalized quantities $\langle 1^2 \rangle^{\overline{\rm MS}}$ [cf. Eq. (43)], $\langle \xi^2 \rangle^{\overline{\rm MS}}$ and $a_2^{\overline{\rm MS}}$ [cf. Eq. (40)]. For each ensemble, the final error budget has to encompass the statistical errors coming from the determination of the bare quantities on the lattice, the systematic uncertainties due to the choice of the fit range,

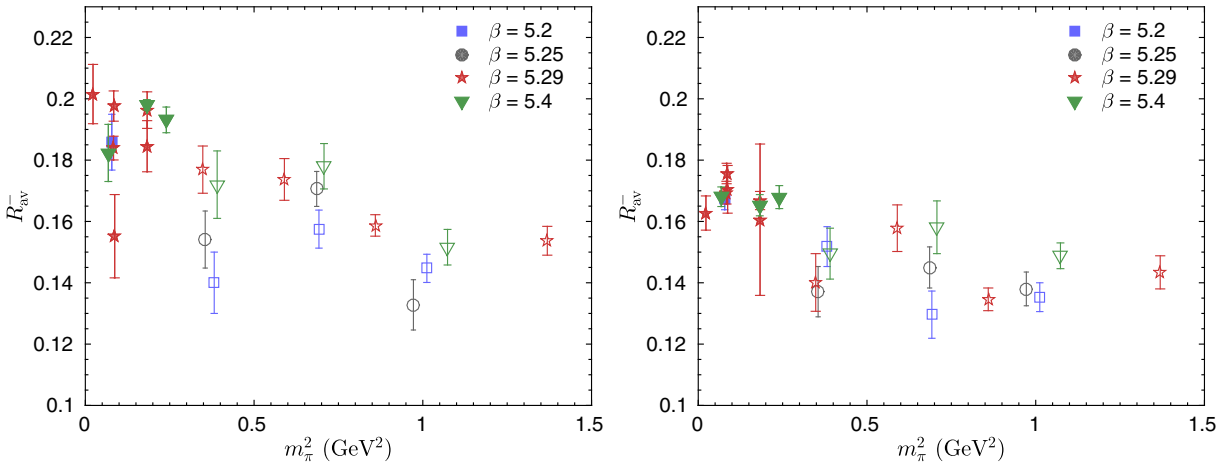

FIG. 2 (color online). Bare results for $R_{\rm av}^{-}$ from this paper (filled symbols) and from [26] (open symbols) for the two interpolators J_{45} (left panel) and J_5 (right panel).

and the errors of the renormalization constants. The ensuing extrapolation to the physical pion mass and eventually to the continuum will introduce further uncertainties. In order to include the errors coming from the renormalization constants we proceed as already indicated at the end of Sec. IV. For every fit choice in Table II, we use the renormalization factors ζ_{11}, ζ_{12}, ζ_{22} resulting from this fit to compute the renormalized quantities from the bare ratios $R^{\pm}_{\rm av}$ according to Eqs. (40) and (43), taking the correlations between $R^{+}_{\rm av}$ and $R^{-}_{\rm av}$ into account. The central value is then taken from the first fit choice, and the error due to the renormalization constants is determined from the differences with the other fit choices, as described in Sec. IV. In the following plots we show the central values together with their statistical errors, while the errors coming from the renormalization constants are not included, but are given in the Tables.

We start by presenting our results for $\langle 1^2\rangle^{\overline{\rm MS}}$. In the continuum limit, this quantity should be one for all pion masses. Results for all ensembles are presented in Table VIII. In Fig. 3, $\langle 1^2\rangle^{\overline{\rm MS}}$ is plotted for the three available lattice spacings using data for $m_\pi L \sim 3.4$–3.8 and $m_\pi \sim 260$–294 MeV (or $m_\pi \sim 280$ MeV for short; the mass dependence is rather weak).

We also show an extrapolation to the continuum limit assuming a linear dependence on a^2. We see that the result is consistent with unity within errors:

$$\langle 1^2\rangle^{\overline{\rm MS}}_{a\to 0} = 0.9963(186)(51). \tag{58}$$

Here the first error is statistical, and the second error accounts for the uncertainty due to the renormalization factors, estimated as described at the end of Sec. IV. It might be surprising that an extrapolation linear in a^2 works so well although our operators are not $O(a)$-improved. However, the covariant derivatives in the operator $\mathcal{O}^{+}_{4jk}$ do not introduce $O(a)$ lattice artifacts, at least at tree level, and the $O(a)$ artifacts in $\mathcal{O}_4$ should cancel to some extent between the numerator and the denominator in the ratio (43). An extrapolation linear in a looks less stable due to the rather small range of a-values and yields a result which is a few percent larger.

Note that for $a^2 \sim 5\times 10^{-3}$ fm^2 corresponding to $\beta = 5.29$, where most of our data are collected, we obtain, e.g., at $m_\pi = 294$ MeV on a $32^3\times 64$-lattice

$$\langle 1^2\rangle^{\overline{\rm MS}}_{a\sim 0.07\ {\rm fm}} = 0.9402(66)(54). \tag{59}$$

The deviation from unity is only 6%, however, it results in a 25%–30% increase in the value of $a_2^{\overline{\rm MS}}$ at the same lattice spacing, calculated using Eq. (45) instead of the continuum relation in Eq. (44).

The results for $\langle \xi^2\rangle^{\overline{\rm MS}}$ and $a_2^{\overline{\rm MS}}$ are given in Tables IX and X, where the first error is statistical and the second comes from the uncertainty in the determination of the renormalization constants. Ideally, one would now take the infinite volume limit, perform the continuum extrapolation at fixed pion masses and finally extrapolate to the physical mass, if it is not included in the range of simulated masses. Unfortunately, our present set of data does not allow us to perform all three extrapolations in a controlled way.

We can however study the finite size effects using the data at $\beta = 5.29$, $\kappa = 0.13620$ ($m_\pi \sim 425$ MeV) and $\kappa = 0.13632$ ($m_\pi \sim 290$ MeV), where we have two and three volumes, respectively. In Fig. 4 we plot $a_2^{\overline{\rm MS}}$ and $\langle \xi^2\rangle^{\overline{\rm MS}}$ versus $m_\pi L$

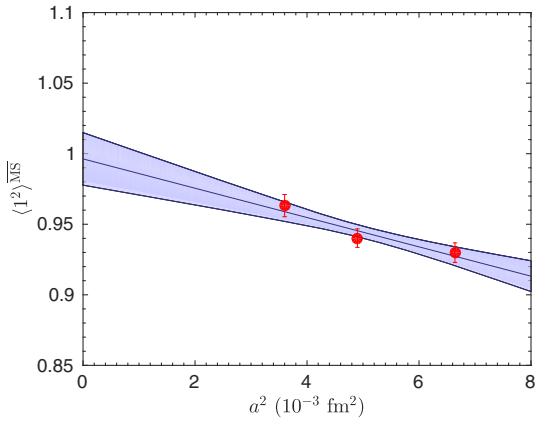

FIG. 3 (color online). $\langle 1^2\rangle^{\overline{\rm MS}}$ as a function of the lattice spacing a for ensembles with $m_\pi L \sim 3.4$–3.8 and $m_\pi \sim 280$ MeV. Only statistical errors are shown.

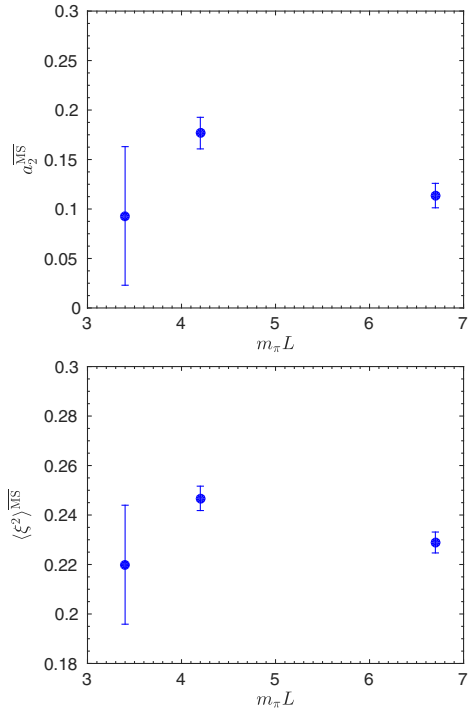

FIG. 4 (color online). Renormalized results $a_2^{\overline{\rm MS}}$ (upper panel) and $\langle \xi^2\rangle^{\overline{\rm MS}}$ (lower panel) as a function of $m_\pi L$ for ensembles with $\beta = 5.29$ and $m_\pi \sim 290$ MeV. Only statistical errors are shown.

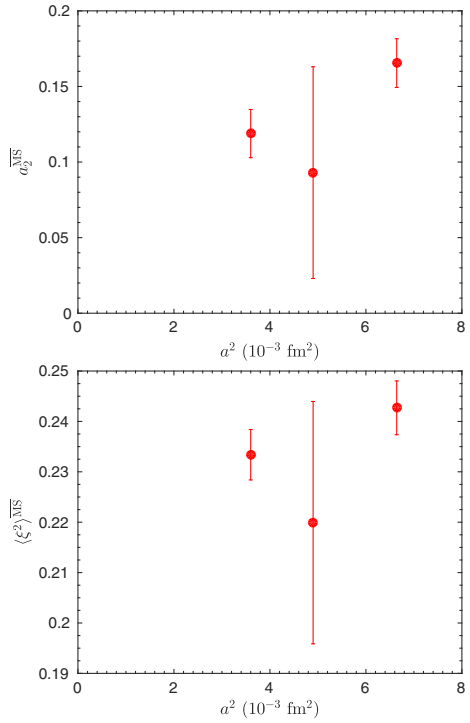

FIG. 5 (color online). Lattice spacing dependence of $a_2^{\overline{\rm MS}}$ (upper panel) and $\langle\xi^2\rangle^{\overline{\rm MS}}$ (lower panel) for $m_\pi \sim 280$ MeV and $m_\pi L \sim 3.4$–3.8. Only statistical errors are shown.

for $m_\pi \sim 290$ MeV and see that there are indications of nonnegligible effects. In leading order chiral perturbation theory, on the other hand, there are no finite volume correction terms, as follows from the results in Ref. [48].

Similarly, we use our ensembles at $m_\pi \sim 280$ MeV and $m_\pi \sim 425$ MeV, where we have three and two different lattice spacings, respectively, to study discretization effects. Results for $a_2^{\overline{\rm MS}}$ and $\langle\xi^2\rangle^{\overline{\rm MS}}$ are shown in Fig. 5. Unfortunately, with only three lattice spacings at hand and relatively large statistical errors, it is impossible to perform a reliable continuum extrapolation.

According to Ref. [48], $\langle\xi^2\rangle^{\overline{\rm MS}}$, and hence also $a_2^{\overline{\rm MS}}$, do not contain chiral logarithms, at least to one-loop order. Therefore we assume a linear dependence on m_π^2 for the extrapolation in the pion mass to the physical value. Since the ensemble with the lightest pion is already very close to the physical point, the chiral extrapolation is reliable. As our lattice spacings do not vary that much, and a proper continuum extrapolation of $\langle\xi^2\rangle^{\overline{\rm MS}}$ and $a_2^{\overline{\rm MS}}$ cannot be attempted, we include results from all lattice spacings, but take into account only the data for the largest volume, where different volumes are available. The resulting extrapolations of $a_2^{\overline{\rm MS}}$ and $\langle\xi^2\rangle^{\overline{\rm MS}}$ to the physical pion mass are plotted in Fig. 6. As in these fits χ^2/dof is greater than one, we follow the procedure advocated by the Particle Data Group [49] and multiply the errors by $\sqrt{\chi^2/\text{dof}}$. As before, errors coming from the renormalization constants are not included in the plot. We perform an extrapolation for every fit choice given in Table II and compute the error of the final number caused by the uncertainties of the renormalization factors from the differences of the extrapolated results as indicated at the end of Sec. IV.

From this procedure we find our final results

$$\langle\xi^2\rangle^{\overline{\rm MS}} = 0.2361(41)(39),$$
$$a_2^{\overline{\rm MS}} = 0.1364(154)(145) \qquad (60)$$

at the scale $\mu = 2$ GeV. They can be compared with the earlier lattice calculations [26,27]

$$\langle\xi^2\rangle^{\overline{\rm MS}} = 0.269(39), \qquad a_2^{\overline{\rm MS}} = 0.201(114),$$
$$\langle\xi^2\rangle^{\overline{\rm MS}} = 0.28(1)(2), \qquad a_2^{\overline{\rm MS}} = 0.233(29)(58), \qquad (61)$$

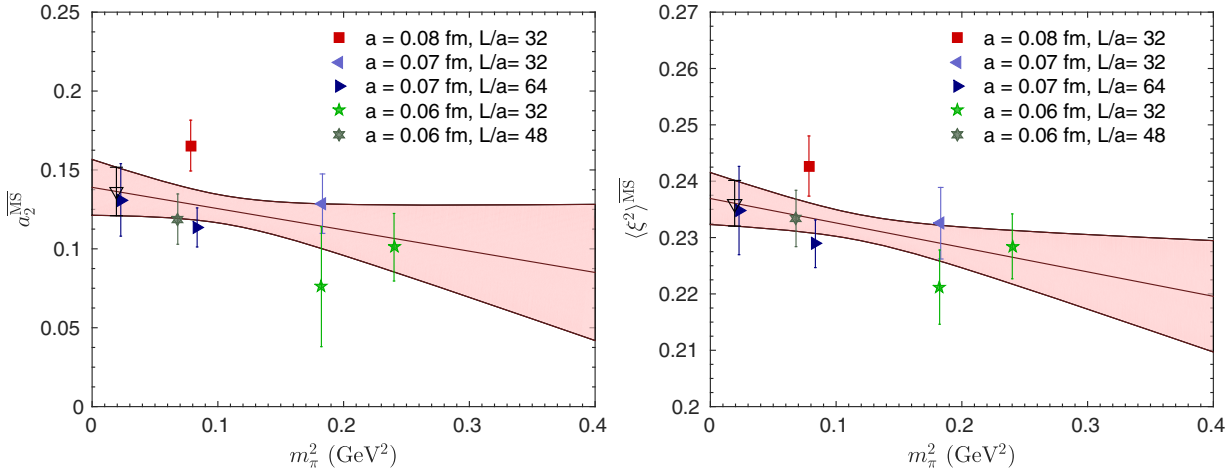

FIG. 6 (color online). Extrapolation to the physical pion mass for $a_2^{\overline{\rm MS}}$ (left panel) and $\langle\xi^2\rangle^{\overline{\rm MS}}$ (right panel). The open triangle represents the extrapolated value. Only statistical errors are shown.

where, for [27], we have quoted the result for $\langle\xi^2\rangle^{\overline{\rm MS}}$ on their larger lattice and used the continuum relation in Eq. (44) to calculate the corresponding value of the second Gegenbauer moment $a_2^{\overline{\rm MS}}$.

It should, however, be kept in mind that all these numbers were obtained on lattices with lattice spacings between 0.06 and 0.08 fm. The investigation of discretization effects for $\langle\xi^2\rangle^{\overline{\rm MS}}$ and $a_2^{\overline{\rm MS}}$ will remain a challenge for future studies.

VII. CONCLUSIONS AND OUTLOOK

We have presented the most accurate, up to now, lattice determination of the second moment of the pion distribution amplitude using two flavors of dynamical (clover) fermions on lattices of different volumes and pion masses down to almost the physical value. So the chiral extrapolation *per se* does not seem to be an issue. Also the omission of strange quarks should not be of great importance. However, the statistical fluctuations of the lattice matrix elements of operators with derivatives are large for small pion masses and require averaging over a large number of configurations in order to obtain phenomenologically relevant precision. We found that the signal can be somewhat improved by using the variational method with the two interpolators corresponding to the pseudoscalar and axial-vector currents.

The main difference of this paper from the previous studies [26,27] is the nonperturbative evaluation of the full 2×2 mixing matrix of the operators with two derivatives. In the framework of Ref. [26] the nonperturbative mixing coefficient turns out to be of the same sign but up to 1 order of magnitude larger than the same coefficient computed perturbatively. This observation underlines the necessity of nonperturbative renormalization, at least at the presently reachable β-values.

Still, some uncertainty in the renormalization factors remains. It is dominated by the uncertainty in the conversion factors connecting the RI'-SMOM scheme to the $\overline{\rm MS}$ scheme, which are calculated in continuum perturbation theory and are known to two-loop accuracy [35,36]. A three-loop calculation is, therefore, needed in order to further reduce the renormalization uncertainty and would be extremely welcome.

In our paper we have also emphasized the importance of using the corrected relation Eq. (45) between $\langle\xi^2\rangle^{\overline{\rm MS}}$ and $a_2^{\overline{\rm MS}}$ for finite lattice spacing, instead of the continuum relation in Eq. (44), due to discretization errors in derivatives that lead to a violation of the product rule. This effect is studied in detail.

From our data we cannot exclude significant discretization effects in $\langle\xi^2\rangle^{\overline{\rm MS}}$ and $a_2^{\overline{\rm MS}}$, but a quantitative study requires simulations at smaller lattice spacings of the order of $a\sim 0.04$ fm, which are presently not available to us. Such lattices will be generated in the future within the CLS effort [50]. This will be a major step towards the calculation of the second moment of the pion DA with fully controllable accuracy. As a final remark, we note that the somewhat smaller value of $a_2^{\overline{\rm MS}}$ obtained in this paper seems to be favored by the phenomenological studies of form factors in the framework of light-cone sum rules, see, e.g., Refs. [7,9,11–13].

ACKNOWLEDGMENTS

This work has been supported in part by the Deutsche Forschungsgemeinschaft (SFB/TR 55) and the European Union under the Grant Agreement No. IRG 256594. The computations were performed on the QPACE systems of the SFB/TR 55, Regensburg's Athene HPC cluster, the SuperMUC system at the LRZ/Germany and Jülich's JUGENE using the CHROMA software system [51] and the BQCD software [52] including improved inverters [53,54]. We thank John Gracey for helpful discussions about renormalization issues and the UKQCD collaboration for giving us permission to use some of their gauge field configurations.

APPENDIX: BARE AND RENORMALIZED RESULTS BY THE ENSEMBLE

The following Tables V, VI, VII, VIII, IX, and X summarize the results obtained for each gauge field ensemble separately.

TABLE V. Bare results for $R_{\rm av}^{\pm}$ using J_5 as interpolator.

β	κ_l	Size	Fit range	$R_{\rm av}^{-}$	χ^2/dof	Fit range	$R_{\rm av}^{+}$	χ^2/dof
5.20	0.13596	$32^3\times 64$	3–14	0.1674(36)	0.67	9–19	0.6013(46)	6.67
5.29	0.13620	$24^3\times 48$	8–12	0.161(25)	0.47	7–12	0.5792(97)	4.44
5.29	0.13620	$32^3\times 64$	3–14	0.1668(30)	0.73	11–20	0.6187(52)	7.73
5.29	0.13632	$32^3\times 64$	3–17	0.1705(78)	0.72	9–15	0.602(11)	7.76
5.29	0.13632	$40^3\times 64$	3–18	0.1756(33)	1.51	10–25	0.6213(36)	5.38
5.29	0.13632	$64^3\times 64$	7–15	0.1694(37)	0.82	15–26	0.6343(22)	6.67
5.29	0.13640	$64^3\times 64$	5–20	0.1627(56)	0.76	17–25	0.6421(61)	6.00
5.40	0.13640	$32^3\times 64$	3–15	0.1679(38)	0.59	14–25	0.654(14)	3.83
5.40	0.13647	$32^3\times 64$	3–15	0.1653(35)	1.04	15–22	0.657(21)	2.78
5.40	0.13660	$48^3\times 64$	3–15	0.1681(32)	0.81	15–25	0.6467(57)	4.22

TABLE VI. Bare results for $R_{\mathrm{av}}^{\pm}$ using J_{45} as interpolator.

β	κ_l	Size	Fit range	R_{av}^{-}	χ^2/dof	Fit range	R_{av}^{+}	χ^2/dof
5.20	0.13596	$32^3 \times 64$	10–16	0.1859(91)	1.57	13–19	0.6354(72)	1.29
5.29	0.13620	$24^3 \times 48$	7–13	0.1845(83)	1.08	10–15	0.680(12)	0.92
5.29	0.13620	$32^3 \times 64$	10–15	0.1963(60)	0.13	18–24	0.617(10)	1.86
5.29	0.13632	$32^3 \times 64$	9–15	0.155(14)	0.25	12–20	0.660(13)	0.67
5.29	0.13632	$40^3 \times 64$	8–15	0.1976(49)	0.83	17–24	0.6441(74)	1.19
5.29	0.13632	$64^3 \times 64$	10–25	0.1839(39)	1.59	16–30	0.6394(23)	1.64
5.29	0.13640	$64^3 \times 64$	10–19	0.2015(97)	0.77	20–30	0.6321(67)	0.37
5.40	0.13640	$32^3 \times 64$	7–15	0.1931(42)	0.41	16–25	0.682(13)	0.77
5.40	0.13647	$32^3 \times 64$	3–13	0.1980(17)	0.59	17–22	0.682(17)	0.22
5.40	0.13660	$48^3 \times 64$	14–20	0.1823(93)	0.60	19–29	0.6640(73)	0.52

TABLE VII. Bare results for $R_{\mathrm{av}}^{\pm}$ using the variational method with the interpolators J_{45}, J_5.

β	κ	Size	Fit range	R_{av}^{-}	χ^2/dof	Fit range	R_{av}^{+}	χ^2/dof
5.20	0.13596	$32^3 \times 64$	3–16	0.1813(27)	0.63	10–19	0.6142(46)	0.52
5.29	0.13620	$24^3 \times 48$	3–13	0.1660(52)	1.01	5–13	0.6039(54)	0.38
5.29	0.13620	$32^3 \times 64$	4–16	0.1775(32)	0.52	9–16	0.6303(35)	0.41
5.29	0.13632	$32^3 \times 64$	6–16	0.1710(120)	0.63	5–16	0.6289(44)	0.35
5.29	0.13632	$40^3 \times 64$	2–23	0.1838(24)	1.52	14–24	0.6226(56)	0.40
5.29	0.13632	$64^3 \times 64$	2–22	0.1761(21)	0.85	8–25	0.6353(14)	0.93
5.29	0.13640	$64^3 \times 64$	2–20	0.1790(39)	0.78	10–20	0.6350(30)	1.35
5.40	0.13640	$32^3 \times 64$	2–14	0.1773(27)	0.55	13–20	0.657(11)	0.45
5.40	0.13647	$32^3 \times 64$	2–16	0.1742(22)	1.03	16–22	0.662(25)	0.26
5.40	0.13660	$48^3 \times 64$	2–16	0.1794(24)	0.80	15–25	0.6534(53)	0.30

TABLE VIII. Results for $\langle 1^2 \rangle^{\overline{\mathrm{MS}}}(\mu = 2\ \mathrm{GeV})$ using the variational method with the interpolators J_{45}, J_5. The first error corresponds to the statistical fluctuations, and the second to the contribution from the uncertainty in the determination of the renormalization constants.

β	κ	Size	$\langle 1^2 \rangle^{\overline{\mathrm{MS}}}(\mu = 2\ \mathrm{GeV})$
5.20	0.13596	$32^3 \times 64$	0.9298(70)(56)
5.29	0.13620	$24^3 \times 48$	0.9028(81)(52)
5.29	0.13620	$32^3 \times 64$	0.9422(53)(55)
5.29	0.13632	$32^3 \times 64$	0.9402(66)(54)
5.29	0.13632	$40^3 \times 64$	0.9308(84)(54)
5.29	0.13632	$64^3 \times 64$	0.9498(20)(55)
5.29	0.13640	$64^3 \times 64$	0.9494(44)(55)
5.40	0.13640	$32^3 \times 64$	0.9690(159)(51)
5.40	0.13647	$32^3 \times 64$	0.9757(371)(51)
5.40	0.13660	$48^3 \times 64$	0.9632(79)(50)

TABLE IX. Results for $\langle\xi^2\rangle^{\overline{\rm MS}}(\mu = 2\ {\rm GeV})$ using the variational method with the interpolators J_{45}, J_5. The first error corresponds to the statistical fluctuations, and the second to the contribution from the uncertainty in the determination of the renormalization constants.

β	κ	Size	$\langle\xi^2\rangle^{\overline{\rm MS}}(\mu = 2\ {\rm GeV})$
5.20	0.13596	$32^3 \times 64$	0.2427(53)(28)
5.29	0.13620	$24^3 \times 48$	0.2147(103)(42)
5.29	0.13620	$32^3 \times 64$	0.2325(63)(42)
5.29	0.13632	$32^3 \times 64$	0.2199(240)(45)
5.29	0.13632	$40^3 \times 64$	0.2467(49)(38)
5.29	0.13632	$64^3 \times 64$	0.2289(42)(44)
5.29	0.13640	$64^3 \times 64$	0.2348(78)(42)
5.40	0.13640	$32^3 \times 64$	0.2284(58)(49)
5.40	0.13647	$32^3 \times 64$	0.2212(66)(51)
5.40	0.13660	$48^3 \times 64$	0.2334(50)(48)

TABLE X. Results for $a_2^{\overline{\rm MS}}(\mu = 2\ {\rm GeV})$ using the variational method with the interpolators J_{45}, J_5. The first error corresponds to the statistical fluctuations, and the second to the contribution from the uncertainty in the determination of the renormalization constants.

β	κ	Size	$a_2^{\overline{\rm MS}}(\mu = 2\ {\rm GeV})$
5.20	0.13596	$32^3 \times 64$	0.1654(161)(113)
5.29	0.13620	$24^3 \times 48$	0.0996(304)(152)
5.29	0.13620	$32^3 \times 64$	0.1286(188)(153)
5.29	0.13632	$32^3 \times 64$	0.0930(700)(161)
5.29	0.13632	$40^3 \times 64$	0.1767(160)(141)
5.29	0.13632	$64^3 \times 64$	0.1136(124)(158)
5.29	0.13640	$64^3 \times 64$	0.1310(230)(154)
5.40	0.13640	$32^3 \times 64$	0.1010(214)(169)
5.40	0.13647	$32^3 \times 64$	0.0760(380)(176)
5.40	0.13660	$48^3 \times 64$	0.1188(159)(164)

[1] V. L. Chernyak and A. R. Zhitnitsky, Asymptotic behavior of hadron form-factors in quark model, JETP Lett. **25**, 510 (1977); Asymptotics of hadronic form-factors in the quantum chromodynamics, Sov. J. Nucl. Phys. **31**, 544 (1980); V. L. Chernyak, A. R. Zhitnitsky, and V. G. Serbo, Asymptotic hadronic form-factors in quantum chromodynamics, JETP Lett. **26**, 594 (1977); Calculation of asymptotics of the pion electromagnetic form-factor in the QCD perturbation theory, Sov. J. Nucl. Phys. **31**, 552 (1980).

[2] A. V. Radyushkin, Deep elastic processes of composite particles in field theory and asymptotic freedom, arXiv: hep-ph/0410276 (English translation); A. V. Efremov and A. V. Radyushkin, Asymptotical behavior of pion electromagnetic form-factor in QCD, Theor. Math. Phys. **42**, 97 (1980); Factorization and asymptotical behavior of pion form-factor in QCD, Phys. Lett. B **94**, 245 (1980).

[3] G. P. Lepage and S. J. Brodsky, Exclusive processes in quantum chromodynamics: Evolution equations for hadronic wave functions and the form-factors of mesons, Phys. Lett. B **87**, 359 (1979); Exclusive processes in perturbative quantum chromodynamics, Phys. Rev. D **22**, 2157 (1980).

[4] B. Aubert *et al.* (*BABAR* Collaboration), Measurement of the $\gamma\gamma^* \to \pi^0$ transition form factor, Phys. Rev. D **80**, 052002 (2009).

[5] S. Uehara *et al.* (Belle Collaboration), Measurement of $\gamma\gamma^* \to \pi^0$ transition form factor at Belle, Phys. Rev. D **86**, 092007 (2012).

[6] A. V. Radyushkin, Shape of pion distribution amplitude, Phys. Rev. D **80**, 094009 (2009).

[7] S. S. Agaev, V. M. Braun, N. Offen, and F. A. Porkert, Light cone sum rules for the $\pi^0\gamma^*\gamma$ form factor revisited, Phys. Rev. D **83**, 054020 (2011).

[8] A. P. Bakulev, S. V. Mikhailov, A. V. Pimikov, and N. G. Stefanis, Comparing antithetic trends of data for the pion-photon transition form factor, Phys. Rev. D **86**, 031501 (2012).

[9] S. S. Agaev, V. M. Braun, N. Offen, and F. A. Porkert, Belle data on the $\pi^0\gamma^*\gamma$ form factor: A game changer?, Phys. Rev. D **86**, 077504 (2012).

[10] V. L. Chernyak and S. I. Eidelman, Hard exclusive two photon processes in QCD, Prog. Part. Nucl. Phys. **80**, 1 (2015).

[11] P. Ball and R. Zwicky, New results on $B \to \pi, K, \eta$ decay form factors from light-cone sum rules, Phys. Rev. D **71**, 014015 (2005).

[12] G. Duplancic, A. Khodjamirian, Th. Mannel, B. Melić, and N. Offen, Light-cone sum rules for $B \to \pi$ form factors revisited, J. High Energy Phys. 04 (2008) 014.

[13] A. Khodjamirian, T. Mannel, N. Offen, and Y.-M. Wang, $B \to \pi\ell\nu_l$ width and $|V_{ub}|$ from QCD light-cone sum rules, Phys. Rev. D **83**, 094031 (2011).

[14] I. I. Balitsky, V. M. Braun, and A. V. Kolesnichenko, $\Sigma^+ \to p\gamma$ decay in QCD, Sov. J. Nucl. Phys. **44**, 1028 (1986); Radiative decay $\Sigma^+ \to p\gamma$ in quantum chromodynamics, Nucl. Phys. **B312**, 509 (1989).

[15] V. L. Chernyak and I. R. Zhitnitsky, B meson exclusive decays into baryons, Nucl. Phys. **B345**, 137 (1990).

[16] M. Beneke, G. Buchalla, M. Neubert, and C. T. Sachrajda, QCD Factorization for $B \to \pi\pi$ Decays: Strong Phases and CP Violation in the Heavy Quark Limit, Phys. Rev. Lett. **83**, 1914 (1999).

[17] M. Beneke and M. Neubert, QCD factorization for $B \to PP$ and $B \to PV$ decays, Nucl. Phys. **B675**, 333 (2003).

[18] S. J. Brodsky, Y. Frishman, G. P. Lepage, and C. T. Sachrajda, Hadronic wave functions at short distances and the operator product expansion, Phys. Lett. B **91**, 239 (1980).

[19] Y. M. Makeenko, Conformal operators in quantum chromodynamics, Yad. Fiz. **33**, 842 (1981) [Sov. J. Nucl. Phys. **33**, 440 (1981)].

[20] V. M. Braun, G. P. Korchemsky, and D. Mueller, The uses of conformal symmetry in QCD, Prog. Part. Nucl. Phys. **51**, 311 (2003).

[21] V. L. Chernyak and A. R. Zhitnitsky, Exclusive decays of heavy mesons, Nucl. Phys. **B201**, 492 (1982); **214**, 547(E) (1983).

[22] M. A. Shifman, A. I. Vainshtein, and V. I. Zakharov, QCD and resonance physics. Theoretical foundations, Nucl. Phys. **B147**, 385 (1979).

[23] A. P. Bakulev, S. V. Mikhailov, and N. G. Stefanis, QCD based pion distribution amplitudes confronting experimental data, Phys. Lett. B **508**, 279 (2001); **590**, 309(E) (2004).

[24] A. Khodjamirian, T. Mannel, and M. Melcher, Kaon distribution amplitude from QCD sum rules, Phys. Rev. D **70**, 094002 (2004).

[25] P. Ball, V. M. Braun, and A. Lenz, Higher-twist distribution amplitudes of the K meson in QCD, J. High Energy Phys. 05 (2006) 004.

[26] V. M. Braun *et al.*, Moments of pseudoscalar meson distribution amplitudes from the lattice, Phys. Rev. D **74**, 074501 (2006).

[27] R. Arthur, P. A. Boyle, D. Brömmel, M. A. Donnellan, J. M. Flynn, A. Jüttner, T. D. Rae, and C. T. C. Sachrajda, Lattice results for low moments of light meson distribution amplitudes, Phys. Rev. D **83**, 074505 (2011).

[28] L. Chang, I. C. Cloët, J. J. Cobos-Martinez, C. D. Roberts, S. M. Schmidt, and P. C. Tandy, Imaging Dynamical Chiral Symmetry Breaking: Pion Wave Function on the Light Front, Phys. Rev. Lett. **110**, 132001 (2013).

[29] I. Adachi (Belle II Collaboration), Status of Belle II and SuperKEKB, JINST **9**, C07017 (2014).

[30] V. Braun and D. Mueller, Exclusive processes in position space and the pion distribution amplitude, Eur. Phys. J. C **55**, 349 (2008).

[31] X. Ji, Parton Physics on a Euclidean Lattice, Phys. Rev. Lett. **110**, 262002 (2013).

[32] M. Göckeler, R. Horsley, E.-M. Ilgenfritz, H. Perlt, P. Rakow, G. Schierholz, and A. Schiller, Lattice operators for moments of the structure functions and their transformation under the hypercubic group, Phys. Rev. D **54**, 5705 (1996).

[33] C. Sturm, Y. Aoki, N. H. Christ, T. Izubuchi, C. T. C. Sachrajda, and A. Soni, Renormalization of quark bilinear operators in a momentum-subtraction scheme with a non-exceptional subtraction point, Phys. Rev. D **80**, 014501 (2009).

[34] M. Göckeler *et al.*, Perturbative and nonperturbative renormalization in lattice QCD, Phys. Rev. D **82**, 114511 (2010); **86**, 099903(E) (2012).

[35] J. A. Gracey, RI'/SMOM scheme amplitudes for quark currents at two loops, Eur. Phys. J. C **71**, 1567 (2011).

[36] J. A. Gracey, Amplitudes for the $n = 3$ moment of the Wilson operator at two loops in the RI'/SMOM scheme, Phys. Rev. D **84**, 016002 (2011).

[37] P. Fritzsch, F. Knechtli, B. Leder, M. Marinkovic, S. Schaefer, R. Sommer, and F. Virotta, The strange quark mass and Lambda parameter of two flavor QCD, Nucl. Phys. **B865**, 397 (2012).

[38] G. S. Bali *et al.*, Nucleon mass and sigma term from lattice QCD with two light fermion flavors, Nucl. Phys. **B866**, 1 (2013).

[39] S. Güsken, U. Löw, K.-H. Mütter, R. Sommer, A. Patel, and K. Schilling, Nonsinglet axial vector couplings of the baryon octet in lattice QCD, Phys. Lett. B **227**, 266 (1989).

[40] S. Güsken, A Study of smearing techniques for hadron correlation functions, Nucl. Phys. B, Proc. Suppl. **17**, 361 (1990).

[41] M. Falcioni, M. L. Paciello, G. Parisi, and B. Taglienti, Again on the SU(3) glueball mass , Nucl. Phys. **B251**, 624 (1985).

[42] C. Michael and I. Teasdale, Extracting glueball masses from lattice QCD, Nucl. Phys. **B215**, 433 (1983).

[43] C. Michael, Adjoint sources in lattice gauge theory, Nucl. Phys. **B259**, 58 (1985).

[44] M. Lüscher and U. Wolff, How to calculate the elastic scattering matrix in two-dimensional quantum field theories by numerical simulation, Nucl. Phys. **B339**, 222 (1990).
[45] B. Blossier, M. Della Morte, G. von Hippel, T. Mendes, and R. Sommer, On the generalized eigenvalue method for energies and matrix elements in lattice field theory, J. High Energy Phys. 04 (2009) 094.
[46] R. W. Schiel, The additional interpolators method for variational analysis in lattice QCD, arXiv:1503.02588.
[47] C. Aubin and K. Orginos, A new approach for Delta form factors, AIP Conf. Proc. **1374**, 621 (2011).
[48] J. W. Chen, H. M. Tsai, and K. C. Weng, Model-independent results for SU(3) violation in twist-3 light-cone distribution functions, Phys. Rev. D **73**, 054010 (2006).
[49] K. A. Olive *et al.* (Particle Data Group Collaboration), Review of particle physics, Chin. Phys. C **38**, 090001 (2014).
[50] M. Bruno *et al.*, Simulation of QCD with $N_f = 2 + 1$ flavors of non-perturbatively improved Wilson fermions, J. High Energy Phys. 02 (2015) 043.
[51] R. G. Edwards, and B. Joó (SciDAC and LHPC and UKQCD Collaborations), The Chroma software system for lattice QCD, Nucl. Phys. B, Proc. Suppl. **140**, 832 (2005).
[52] Y. Nakamura and H. Stüben, BQCD–Berlin quantum chromodynamics program, *Proc. Sci.*, LATTICE2010 (2010) 040 [arXiv:1011.0199].
[53] A. Nobile, Solving the Dirac equation on QPACE, *Proc. Sci.*, LATTICE2010 (2010) 034.
[54] M. Lüscher and S. Schaefer, http://cern.ch/luscher/openQCD, 2012.